AMERICAN SOCIETY FOR MICROBIOLOGY | Journal of Virology®

PATHOGENESIS AND IMMUNITY

CD4- and Time-Dependent Susceptibility of HIV-1-Infected Cells to Antibody-Dependent Cellular Cytotoxicity

Wen Shi Lee,[a] Jérémie Prévost,[b,c] Jonathan Richard,[b,c] Reneé M. van der Sluis,[d] Sharon R. Lewin,[d,e] Marzena Pazgier,[f] Andrés Finzi,[b,c,g] Matthew S. Parsons,[a] Stephen J. Kent[a,h,i]

[a]Department of Microbiology and Immunology, Peter Doherty Institute for Infection and Immunity, University of Melbourne, Melbourne, Victoria, Australia
[b]Centre de Recherche du CHUM, Montreal, Quebec, Canada
[c]Département de Microbiologie, Infectiologie et Immunologie, Université de Montréal, Montreal, Quebec, Canada
[d]Peter Doherty Institute for Infection and Immunity, University of Melbourne and Royal Melbourne Hospital, Melbourne, Victoria, Australia
[e]Department of Infectious Diseases, Alfred Hospital and Monash University, Melbourne, Victoria, Australia
[f]Infectious Diseases Division, Uniformed Services University of the Health Sciences, Bethesda, Maryland, USA
[g]Department of Microbiology and Immunology, McGill University, Montreal, Quebec, Canada
[h]Melbourne Sexual Health Centre and Department of Infectious Diseases, Central Clinical School, Monash University, Melbourne, Victoria, Australia
[i]ARC Centre of Excellence in Convergent Bio-Nano Science and Technology, University of Melbourne, Melbourne, Victoria, Australia

ABSTRACT HIV-1-specific antibody-dependent cellular cytotoxicity (ADCC) antibodies within HIV-1-positive (HIV-1$^+$) individuals predominantly target CD4-induced (CD4i) epitopes on HIV-1 envelope glycoprotein (Env). These CD4i epitopes are usually concealed on the surface of infected cells due to CD4 downregulation by the HIV-1 accessory proteins Nef and Vpu. We hypothesized that early-stage infected cells in the process of downregulating CD4 could be more susceptible to ADCC than late-stage infected cells that have fully downregulated CD4. There was significantly higher binding of antibodies within plasma from HIV-1-infected individuals to early-stage infected cells expressing intermediate levels of CD4 (CD4-intermediate cells) than in late-stage infected cells expressing low levels of CD4 (CD4-low cells). However, we noted that HIV-1-uninfected bystander cells and HIV-1-infected cells, at various stages of downregulating CD4, were all susceptible to NK cell-mediated ADCC. Importantly, we observed that the cytolysis of bystander cells and early infected cells in this culture system was driven by sensitization of target cells by inoculum-derived HIV-1 Env or virions. This phenomenon provided Env to target cells prior to *de novo* Env expression, resulting in artifactual ADCC measurements. Future studies should take into consideration the inherent caveats of *in vitro* infection systems and develop improved models to address the potential role for ADCC against cells with nascent HIV-1 infection.

IMPORTANCE An increasing body of evidence suggests that ADCC contributes to protection against HIV-1 acquisition and slower HIV-1 disease progression. Targeting cells early during the infection cycle would be most effective in limiting virus production and spread. We hypothesized that there could be a time-dependent susceptibility of HIV-1-infected cells to ADCC in regard to CD4 expression. We observed NK cell-mediated ADCC of HIV-1-infected cells at multiple stages of CD4 downregulation. Importantly, ADCC of early infected cells appeared to be driven by a previously unappreciated problem of soluble Env and virions from the viral inoculum sensitizing uninfected cells to ADCC prior to *de novo* Env expression. These results have implications for studies examining ADCC against cells with nascent HIV-1 infection.

KEYWORDS ADCC, antibodies, CD4, HIV

Citation Lee WS, Prévost J, Richard J, van der Sluis RM, Lewin SR, Pazgier M, Finzi A, Parsons MS, Kent SJ. 2019. CD4- and time-dependent susceptibility of HIV-1-Infected cells to antibody-dependent cellular cytotoxicity. J Virol 93:e01901-18. https://doi.org/10.1128/JVI.01901-18.

Editor Viviana Simon, Icahn School of Medicine at Mount Sinai

Address correspondence to Stephen J. Kent, skent@unimelb.edu.au.

Received 25 October 2018
Accepted 24 February 2019
Accepted manuscript posted online 6 March 2019
Published 1 May 2019

The elimination of human immunodeficiency virus type 1 (HIV-1)-infected cells through antibody-dependent cellular cytotoxicity (ADCC) represents a potentially useful immune response to integrate into vaccination or curative strategies against HIV-1 infection. Indeed, ADCC has been linked to the partial protection from HIV-1 infection conferred by the RV144 regimen (1) and the protection from pathogenic simian immunodeficiency virus (SIV) challenge conferred to rhesus macaques by a live attenuated SIV vaccine (2). Similarly, ADCC has been shown to impact disease progression in HIV-1-infected humans and SIV-infected macaques (3–5). Despite the prophylactic and therapeutic potential of anti-HIV-1 ADCC, most circulating HIV-1 strains are capable of evading ADCC antibodies predominantly induced during HIV-1 infection or following vaccination. The antibodies capable of triggering ADCC within infected or vaccinated individuals most commonly target CD4-induced (CD4i) epitopes within HIV-1 Env (6–8). Cells infected with most HIV-1 strains, however, evade antibodies targeting CD4i epitopes through the downregulation of cell surface CD4 by the viral Nef and Vpu accessory proteins (9).

Assays utilized to assess evasion of anti-HIV-1 ADCC through Nef- and Vpu-mediated CD4 downregulation have typically employed cells infected for 48 h (6, 9, 10). This raises the question of whether there is a time-dependent susceptibility of HIV-1-infected cells to ADCC in regard to CD4 expression. Are early-stage infected cells that have not fully downregulated CD4 more susceptible to ADCC than late-stage infected cells that have fully downregulated CD4? The potential coexpression of *de novo* Env and CD4 would facilitate the exposure of CD4i epitopes that are highly targeted by ADCC antibodies within HIV-1-infected and vaccinated individuals. On a similar note, the transient exposure of CD4i epitopes on Env during viral entry (preintegration) has also been proposed as a target for ADCC (11, 12). Targeting cells early during the infection cycle, either during viral entry or postintegration before CD4 is fully downregulated, would be most effective in limiting virus production and spread.

While the possibility of time-dependent differential susceptibility to ADCC is a topic that warrants investigation, it is important to note that *in vitro* measurements of anti-HIV-1 ADCC are complicated due to bystander effects that can confound data interpretation. Indeed, HIV-1-infected cell cultures contain soluble gp120 that can bind to uninfected cells and expose CD4i epitopes, allowing CD4i ADCC antibodies to bind and create ideal bystander target cells for effector NK cells (13, 14). It is plausible that a similar phenomenon could result in early HIV-1-infected cells within *in vitro* cultures acquiring ADCC epitopes prior to *de novo* Env expression. As such, it is important to assess time-dependent anti-HIV-1 ADCC early following the infection of target cells to prevent the accumulation of shed gp120. Another potential confounding variable for anti-HIV-1 ADCC measurements is the viral inoculum, which contains both virions and gp120 that could stably bind to CD4 on the surface of cells and reveal CD4i ADCC epitopes as well. In such a situation, the ADCC epitopes would be available in exaggerated quantities to what would be available during the infection of a cell by a single virion. Thus, caution needs to be taken in interpreting the results of experiments assessing the time dependence of anti-HIV-1 ADCC.

Here, we evaluated the temporal susceptibility of HIV-1-infected target cells to ADCC, as well as the antibody specificity involved in the observed responses. Furthermore, we assessed if the detected responses were directed toward *de novo* Env, shed gp120, or inoculum-derived Env that bound to cells during the infection process. We found that while CD4 was not completely downregulated early in infection, there was limited or no *de novo* Env expression at this stage. Our results suggest that inoculum-derived gp120 and virions are major contributors to *in vitro* anti-HIV-1 ADCC responses and that extra care should be taken to infect cells under conditions that more closely reflect natural HIV-1 infection to avoid creating artifactual ADCC susceptibility.

RESULTS

CD4 is progressively downregulated on HIV-1-infected cells. Several studies have shown that ADCC antibodies within serum and plasma from HIV-1-infected or

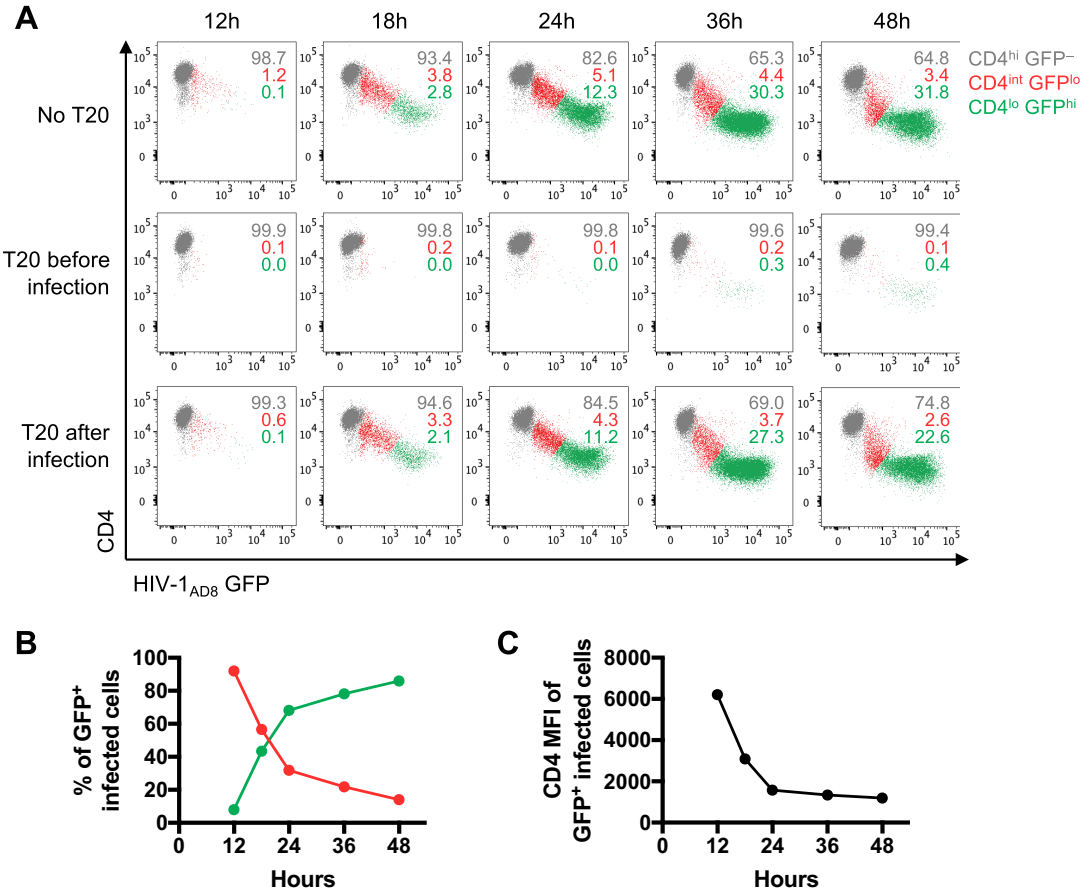

FIG 1 CD4 downregulation and GFP expression over time in CEM cells infected with HIV-1_{AD8}. (A) Flow cytometry scatter plots depicting CD4 and HIV-1_{AD8} (GFP) expression over 12 to 48 h. The top panel shows HIV-1_{AD8}-infected CEM cells in the absence of T20. The middle and bottom panels show CEM cells treated with 10 μg/ml of T20 before or 4 h after spinoculation with HIV-1_{AD8}. The numbers represent the proportions of $CD4^{hi}$ GFP^{-}, $CD4^{int}$ GFP^{lo}, and $CD4^{lo}$ GFP^{hi} cells, as indicated. (B) The proportions of $CD4^{int}$ and $CD4^{lo}$ GFP^{+} infected CEM cells over time. (C) CD4 expression in terms of median fluorescence intensity (MFI) on GFP^{+} infected CEM cells over time. The data in panels B and C were averaged from four independent experiments.

vaccinated individuals predominantly target the CD4-bound conformation of Env (6–8). A potential barrier for these antibodies to recognize HIV-1-infected cells is that CD4i epitopes, exposed when Env binds to CD4, are concealed on infected cells due to the downregulation of CD4 by Nef and Vpu (9). To examine whether a window of opportunity exists for CD4i antibodies to target HIV-1-infected cells before CD4 is fully downregulated, we infected CEM.NKr-CCR5 (CEM) cells with a green fluorescent protein (GFP) reporter HIV-1_{AD8} strain that expresses Nef (under the control of an internal ribosome entry site [IRES]) and Vpu (15). We examined CD4 and GFP expression over time and found that CD4 is progressively downregulated as GFP increases over a period of 12 to 48 h (Fig. 1A, top panel). The cells transition from an uninfected state expressing high levels of CD4 (CD4-high cells, or $CD4^{hi}$) and no GFP (GFP^{-}) to a state expressing intermediate levels of CD4 (CD4-intermediate cells, or $CD4^{int}$) and low levels of GFP early in infection (GFP^{lo}), and finally toward a state expressing low levels of CD4 (CD4-low cells, or $CD4^{lo}$) and high levels of GFP late in infection (GFP^{hi}). The $CD4^{lo}$ GFP^{hi} cells become the predominant population of GFP-positive (GFP^{+}) infected cells over time (Fig. 1B) as CD4 is progressively downregulated (Fig. 1C). To examine the progression of infection in the absence of second rounds of infection, we added the fusion inhibitor T20 4 h after spinoculation with HIV-1_{AD8}. There was very little change in the percentage of cells transitioning to the $CD4^{int}$ GFP^{lo} and $CD4^{lo}$ GFP^{hi} stages at each time point compared to percentages of cells without T20 (Fig. 1A, bottom panel). Since

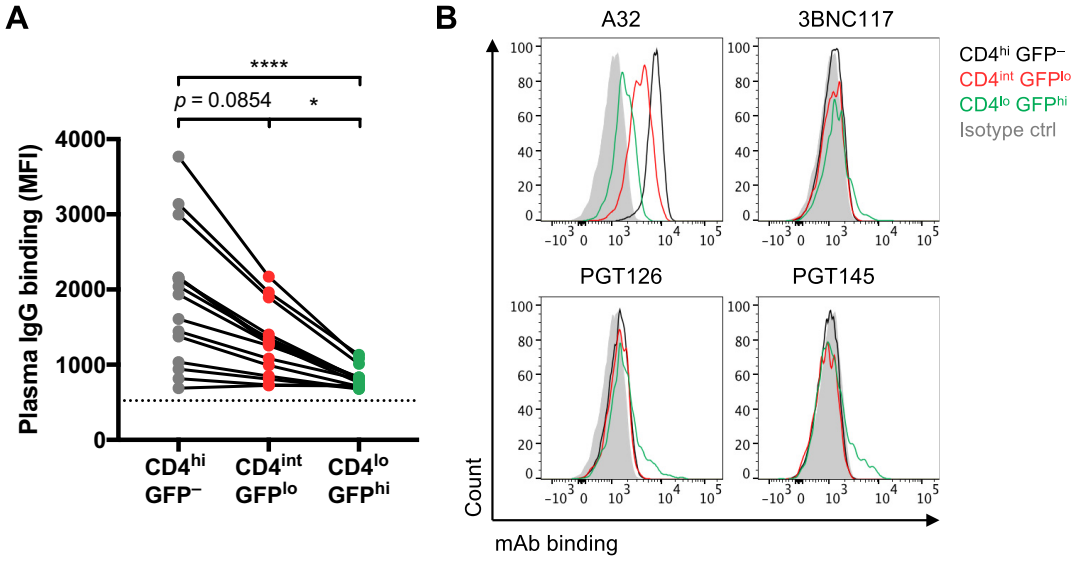

FIG 2 Binding of HIV-1$^+$ plasma antibodies and Env-specific MAbs to HIV-1_{AD8}-infected and uninfected CEM cells. (A) The binding of IgG within HIV-1$^+$ plasma (1:1,000 dilution; $n = 15$ donors) to uninfected CD4^{hi} GFP$^-$ bystanders and CD4^{int} GFP^{lo}, and CD4^{lo} GFP^{hi} infected cells was analyzed by flow cytometry, and results are presented as MFI values. The dotted black line represents plasma IgG binding of an HIV-1$^-$ donor. Statistical analyses between multiple matched groups were performed using the Friedman test followed with Dunn's posttests (*, $P < 0.05$; ****, $P < 0.0001$). (B) The binding of Env-specific MAbs to uninfected CD4^{hi} GFP$^-$, CD4^{int} GFP^{lo}, and CD4^{lo} GFP^{hi} cells, as indicated, was analyzed by flow cytometry. The following Env-specific MAbs were used at 5 μg/ml: A32 (CD4i cluster A), 3BNC117 (CD4 binding site), PGT126 (N332 glycosylation site on the V3 loop), and PGT145 (V1V2 apex). The IgG isotype control was an MAb specific for influenza virus nucleoprotein (D1-11).

T20 was added before a second round of infection could occur, we conclude that the presence of CD4^{int} GFP^{lo} cells at the 36- and 48-h time points was likely due to delayed progression of infection from the initial viral inoculum. As a positive control, cells treated with T20 prior to infection with HIV-1_{AD8} mostly remained uninfected (Fig. 1A, middle panel).

At 20 h postinfection, in the absence of T20, there were similar proportions of early CD4^{int} GFP^{lo} and late CD4^{lo} GFP^{hi} infected cells (Fig. 1B). Thus, we chose the 20-h infection time point for future assays to study whether infected cells can be targeted by ADCC antibodies early in infection.

Recognition of uninfected and HIV-1-infected cells by a panel of Env-specific MAbs and antibodies within HIV-1$^+$ plasma and serum. We hypothesized that CD4^{int} GFP^{lo} infected cells are reflective of cells in the early stages of infection and could be important targets for ADCC antibodies. Since antibodies within plasma from HIV-1-infected and vaccinated individuals predominantly target the CD4-bound conformation of Env (6–8), we next examined whether there would be higher binding of HIV-1$^+$ plasma antibodies to CD4-expressing infected cells than to infected cells that have fully downregulated CD4. Indeed, there was significantly higher binding of plasma IgG antibodies to CD4^{int} GFP^{lo} cells than to CD4^{lo} GFP^{hi} infected cells (median fluorescence intensity [MFI] of 1,280 versus 808; $P < 0.05$) (Fig. 2A).

Previous studies have shown that uninfected bystander CD4$^+$ cells within infected cell cultures can bind gp120 shed from productively infected cells, making them targets for CD4i antibodies within HIV-1$^+$ plasma (13, 14). While it is unlikely that high levels of shed gp120 would be present at this early time point (20 h), soluble gp120 or virions from the inoculum can bind to uninfected bystanders and result in a similar phenomenon. We show that CD4^{hi} GFP$^-$ uninfected cells have even higher levels of HIV-1$^+$ plasma IgG binding than CD4^{int} GFP^{lo} cells (MFI of 1,935 versus 1,280; $P = 0.085$) and CD4^{lo} GFP^{hi} cells (MFI of 1,935 versus 808; $P < 0.0001$) (Fig. 2A).

Polyclonal sera from HIV-1-infected individuals contain a large range of Env-specific antibodies. To more finely dissect the Env epitopes expressed on infected cells, we examined binding of several Env-specific monoclonal antibodies (MAbs) (Fig. 2B). The

nonneutralizing A32 MAb, which binds to a CD4i cluster A epitope on the inner domain of gp120 (11, 16), predominantly recognized the uninfected GFP$^-$ bystanders that have gp120 bound to CD4 on the surface. A32 could bind CD4^{int} GFP^{lo} cells moderately well and even bound to CD4^{lo} GFP^{hi} cells, showing that either CD4 has not been fully downregulated on the CD4^{lo} GFP^{hi} cells or that there may be low levels of CD4i epitopes exposed on cells infected with HIV-1_{AD8} even without CD4 ligation. The broadly neutralizing antibodies (bNAbs) 3BNC117 (CD4-binding site), PGT126 (N332 glycosylation site on the V3 loop), and PGT145 (V1V2 apex) exhibited low levels of binding to CD4^{lo} GFP^{hi} infected cells, where Env is more likely to be in an unliganded, closed conformation. A MAb against influenza virus nucleoprotein (MAb D1-11) served as an isotype control for the staining of Env-specific MAbs (17).

We next assessed Env expression in primary CD4$^+$ T cells infected with the GFP reporter HIV-1_{ADA} strain (9) and stained with a similar panel of MAbs at 48 h postinfection (Fig. 3A). A32 binding was dependent on the level of CD4, with the highest binding to gp120-coated CD4^{hi} GFP$^-$ uninfected bystander cells, moderate binding to CD4^{int} GFP^{lo} cells, and low binding to CD4^{lo} GFP^{hi} cells. The binding of MAb 2G12, specific for a CD4-independent outer domain epitope (18), showed that the uninfected bystanders had higher levels of gp120 than CD4^{int} GFP^{lo} and CD4^{lo} GFP^{hi} cells. In line with the results shown in Fig. 2B, the bNAbs PGT126 and 3BNC117 predominantly recognized CD4^{lo} GFP^{hi} infected cells.

Last, we examined the binding of MAbs and HIV-1$^+$ serum antibodies to primary CD4$^+$ T cells infected with an HIV-1 infectious molecular clone expressing Env from a transmitted/founder virus (CH077.t) at 18 h postinfection using p24 expression as a readout of infectivity (Fig. 3B). The binding of HIV-1$^+$ serum antibodies resembled the binding of A32, with higher binding to CD4^{int} p24$^+$ cells than to CD4^{lo} p24$^+$ cells. The bNAbs PGT126 and PGT151 (gp120-gp41 interface) predominantly recognized CD4^{lo} p24$^+$ cells, with moderate binding to CD4^{int} p24$^+$ cells.

As a control, we also examined the binding of MAbs to cells infected with Nef- and Vpu-deficient HIV-1. Without the antagonism of tetherin by Vpu and the downregulation of CD4 by both Nef and Vpu, these infected cells have high levels of Env and CD4 on the surface, resulting in high levels of binding of all antibodies tested (both CD4i and non-CD4i) (Fig. 3A and B).

CD4-intermediate infected cells are not more susceptible to ADCC than CD4-low infected cells. Having shown that HIV-1$^+$ plasma and serum antibodies preferentially bind CD4^{int} GFP^{lo} cells over CD4^{lo} GFP^{hi} cells, we next examined whether there was higher ADCC against CD4^{int} GFP^{lo} cells. Since uninfected GFP$^-$ bystander cells have been shown to be good targets for ADCC and could confound the measurement of ADCC responses (14), we first sorted HIV-1_{AD8}-infected CEM cells at 20 h postinfection into GFP$^-$, GFP^{lo}, and GFP^{hi} cells to examine ADCC against the three populations independently. We found that the sorted target cells, in the absence of effector NK cells or ADCC antibodies, continued to downregulate CD4 and transition during the 5-h ADCC assay incubation (Fig. 4). Within the sorted GFP$^-$ population, 7.2% transitioned to a CD4^{int} GFP^{lo} state, and 3.1% transitioned to a CD4^{lo} GFP^{hi} state, while 84.4% of the sorted GFP^{lo} population (initially all CD4^{int}) became CD4^{lo} GFP^{hi} in the representative example shown. The sorted GFP^{hi} cells remained CD4^{lo} but continued to express HIV-1 (GFP) during the ADCC assay incubation, increasing in GFP MFI from 14,995 to 31,999 after 5 h. This general pattern of continued CD4 downregulation and GFP expression postsorting was observed across six independent experiments.

We examined ADCC against the sorted populations and calculated ADCC using a reference population (eFluor670-stained uninfected CEM cells) that was spiked into each sample at the end of the ADCC assay incubation (Fig. 5A). We found that all three populations were eliminated by ADCC in an HIV-1-specific manner in contrast to cells incubated with the HIV-1-negative (HIV-1$^-$) plasma control. Although there was higher binding of HIV-1$^+$ plasma antibodies to CD4^{int} GFP^{lo} cells, there was no significant difference in ADCC against the sorted GFP^{lo} or GFP^{hi} cells (median, 15.7% [interquartile range, 12.3% to 31.1%] versus 20.5% [7.9% to 30.5%]; $P = 0.87$) (Fig. 5C).

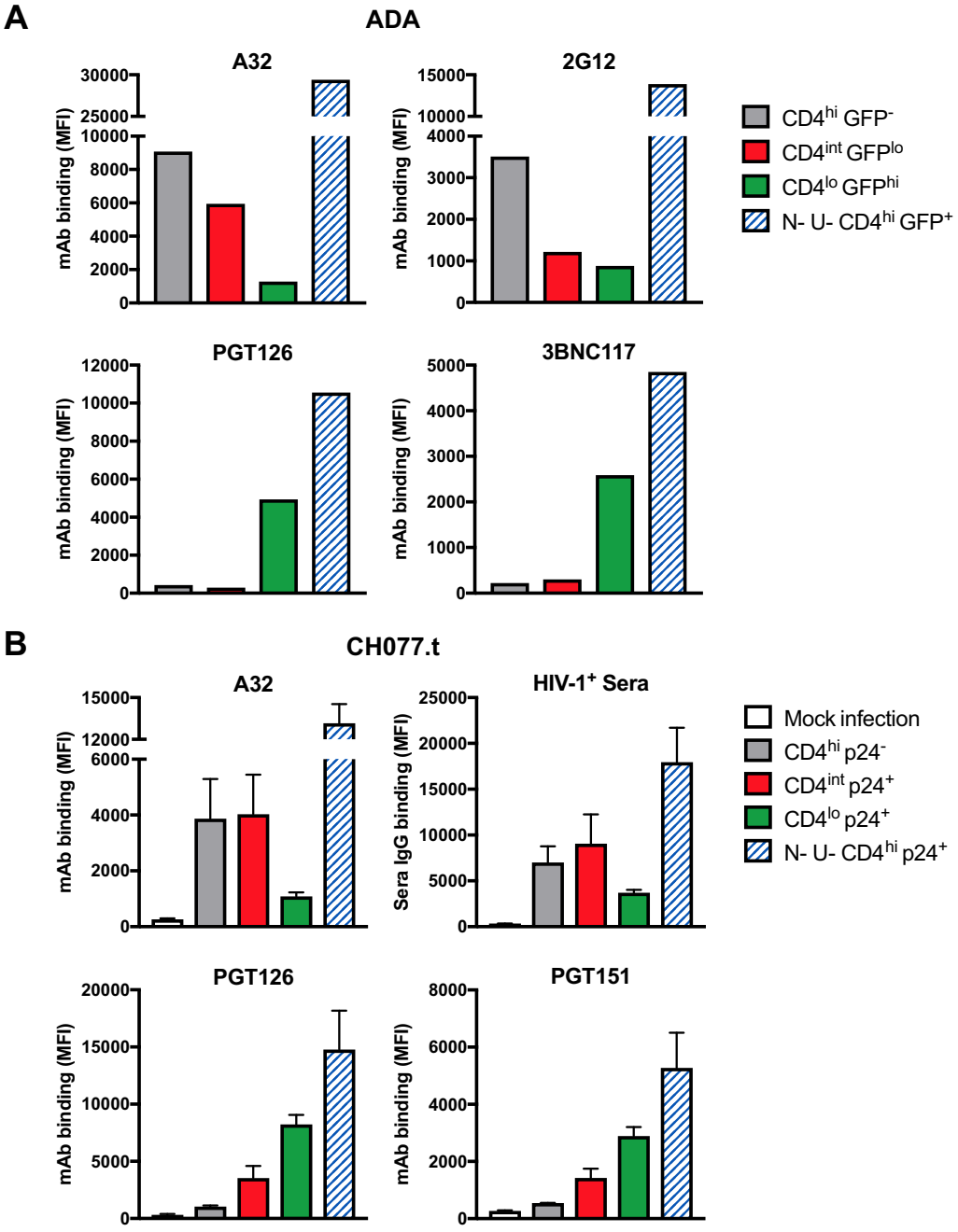

FIG 3 Binding of Env-specific MAbs and HIV-1$^+$ serum antibodies to HIV-1-infected and uninfected primary CD4$^+$ T cells. (A) Primary CD4$^+$ T cells infected with the GFP reporter HIV-1_{ADA} strain were stained at 48 h postinfection with the MAbs A32 (CD4i cluster A), 2G12 (CD4-independent outer domain epitope), PGT126 (N332 glycosylation site on the V3 loop), and 3BNC117 (CD4 binding site) at 5 μg/ml. (B) Primary CD4$^+$ T cells infected with the transmitted/founder HIV-1 infectious molecular clone CH077.t were stained at 18 h postinfection with HIV-1$^+$ serum (1:1,000; $n = 3$) and the MAbs A32, PGT126, and PGT151 (gp120-gp41 interface) at 5 μg/ml. The bar graphs depict mean values obtained from three independent experiments, with error bars showing standard errors of the means. Cell populations are indicated on the figure. The binding of Env-specific MAbs and HIV-1$^+$ serum antibodies was determined using flow cytometry, and results are presented as MFI values. N$^-$ U$^-$, cells infected with Nef- and Vpu-deficient HIV-1.

As the sorted GFP^{lo} cells (initially all CD4^{int}) continued to downregulate CD4 during the 5-h ADCC assay incubation (Fig. 4), it was difficult to determine at which stage (CD4^{int} or CD4^{lo}) the cells were killed. Since a proportion of the apparently uninfected sorted GFP$^-$ cells at 20 h postinfection began to express GFP over the 5-h ADCC incubation (Fig. 4), we could examine ADCC against this population to assess the killing

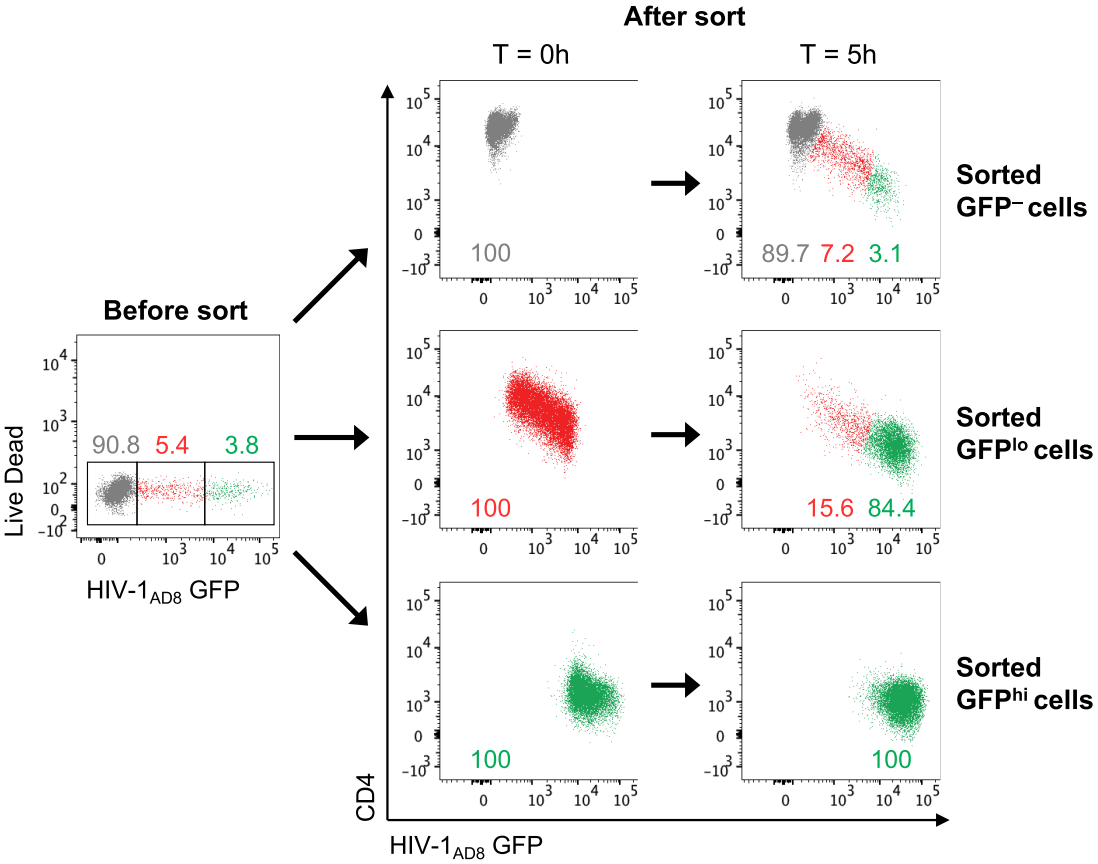

FIG 4 Sorted HIV-1_{AD8}-infected CEM cells continue to downregulate CD4 and express GFP during the 5-h ADCC assay incubation. The left scatter plot depicts the gating strategy utilized to sort HIV-1-infected CEM cells (20 h postinfection) into GFP$^-$, GFP^{lo}, and GFP^{hi} populations. The right panels depict CD4 and GFP expression of the sorted populations directly after the sort (time [*T*] = 0 h) and after the 5-h ADCC assay incubation. All plots in this figure depict the target cells-only samples without any effector NK cells or plasma antibodies. The plots here are representative of six independent experiments.

of cells early during the infection process. We therefore examined ADCC mediated by HIV-1$^+$ plasma antibodies against sorted GFP$^-$ bystander cells that remained uninfected (GFP$^-$) compared to that against the ~10% of cells that became infected (GFP$^+$) during the 5-h ADCC incubation. We found that there was significantly higher ADCC against the cells that became GFP$^+$ than against the cells that remained GFP$^-$ (median, 53.8% [interquartile range, 32% to 83.3%] versus 27.7% [19% to 37.5%]; $P < 0.0001$) (Fig. 5B). This implies that early-stage infected cells could be better targets for ADCC than uninfected bystander cells that have CD4-bound Env.

CD4-induced epitopes are important for ADCC against GFP$^-$ cells and CD4-intermediate infected cells. Since A32-like antibodies against CD4i epitopes are common in HIV-1$^+$ plasma (19), we assessed whether A32 Fabs could block ADCC against HIV-1_{AD8}-infected CEM cells. We first showed that A32 Fabs significantly reduced binding of HIV-1$^+$ plasma IgG against CD4^{hi} GFP$^-$, CD4^{int} GFP^{lo}, and CD4^{lo} GFP^{hi} cells (Fig. 6A). Although binding of HIV-1$^+$ plasma antibodies to CD4^{lo} GFP^{hi} cells was low, this binding could still be blocked with A32 Fabs, suggesting that low levels of CD4i epitopes were still present on the CD4^{lo} GFP^{hi} infected cells. Next, we found that A32 Fabs significantly reduced ADCC against sorted GFP$^-$ and GFP^{lo} cells (Fig. 6B). Some HIV-1$^+$ plasma donors still had relatively high ADCC even after the A32 epitope was blocked, suggesting that these donors have ADCC antibodies that can recognize other epitopes on Env. Last, we found that A32 Fabs did not significantly reduce ADCC against sorted GFP^{hi} cells.

ADCC against infected cells at an early stage is due to CD4-bound gp120 or virions that originated from the viral inoculum. Shed gp120 in infected cell cultures

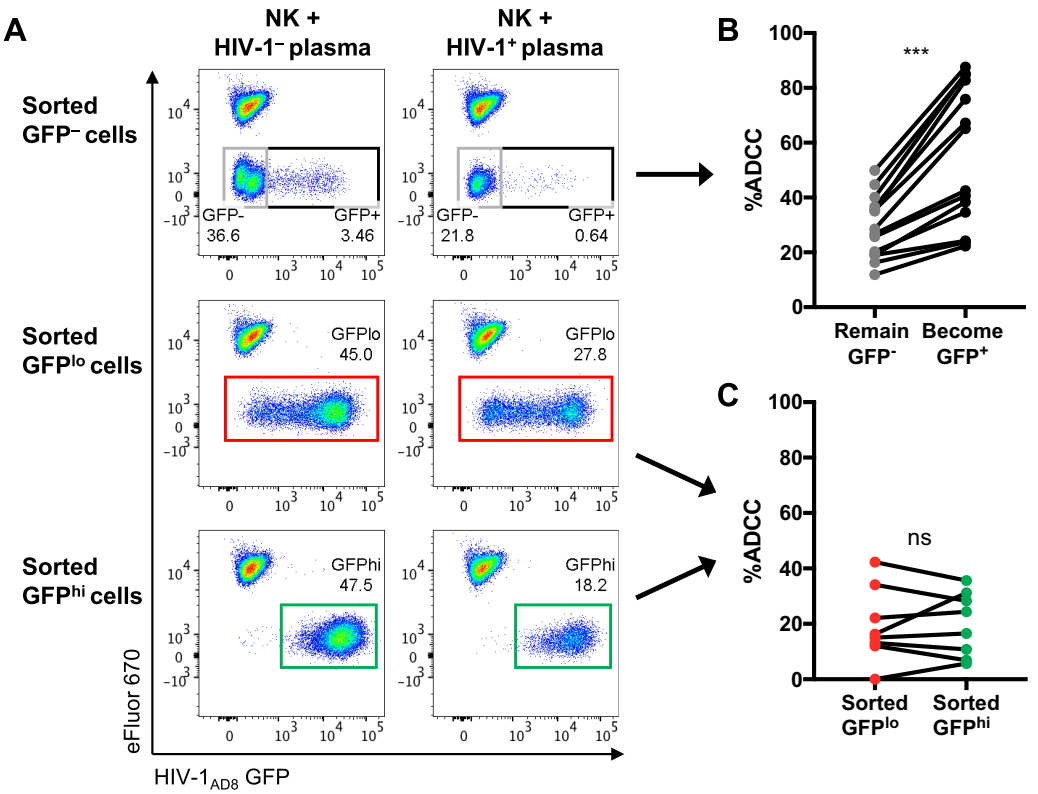

FIG 5 ADCC against HIV-1_{AD8}-infected CEM cells sorted into GFP⁻, GFP^{lo}, and GFP^{hi} populations. (A) Representative scatter plots showing elimination of the sorted target cells in the presence of effector NK cells with HIV-1⁺ plasma compared to NK cells with HIV-1⁻ plasma. Uninfected CEM cells stained with the cell proliferation dye eFluor 670 (eFluor 670⁺ GFP⁻) were spiked into each sample at the end of the 5-h ADCC assay incubation to serve as a reference population to calculate percent ADCC of the sorted target cells. (B) ADCC mediated by HIV-1⁺ plasma (1:1,000; $n = 14$) against sorted GFP⁻ cells that remained GFP⁻ or became GFP⁺ after the 5-h assay incubation. (C) ADCC mediated by HIV-1⁺ plasma (1:1,000; $n = 8$) against sorted GFP^{lo} and GFP^{hi} cells. Statistical analyses between matched pairs were performed with a Wilcoxon signed-rank test (ns, not significant; ***, $P < 0.001$).

can give rise to artifactual ADCC results if the assay measures effector cell activation or killing of total target cells (i.e., uninfected bystanders plus infected cells) (14). Another source of Env that can bind to CD4 on uninfected bystanders is the viral inoculum. To examine the possibility that sources of Env in the viral inoculum were confounding our results, we examined ADCC against HIV-1-exposed CEM cells in the presence of a CD4-blocking antibody or an isotype control. The HIV-1-exposed CEM cells were spinoculated with HIV-1_{AD8} for 1 h as for the above-described experiments, washed to remove any unbound gp120 or virions, and immediately used as targets for the ADCC assay without any prior incubation for viral replication to occur. In contrast to the low level of killing of mock-infected cells, we found that HIV-1-exposed cells were significantly killed by ADCC (median, 3.2% [interquartile range, 1.8% to 5.9%] versus 15.7% [11.6% to 19.6%]; $P < 0.05$) (Fig. 7A), showing that HIV-1-exposed cells can be targets for ADCC even without viral replication. The sensitization of target cells to ADCC by the viral inoculum was CD4 dependent as blocking CD4 prior to spinoculation significantly reduced ADCC (median for the isotype control, 15.7% [interquartile range, 11.6% to 19.6%] versus CD4-blocked cells, 2.6% [0.6% to 7.5%]; $P < 0.05$). Of note, spinoculation of CEM cells with monomeric gp120, rather than with viral preparations, also resulted in high levels of ADCC mediated by HIV-1⁺ plasma (data not shown). We next stained HIV-1-exposed cells for p24 expression to examine whether HIV-1 virions could be detected on the cell surface (Fig. 7D). Immediately after spinoculation with HIV-1_{AD8}, 68.3% of CD4^{hi} GFP⁻ uninfected cells were p24⁺ in contrast to mock-infected cells that were all p24⁻, reflecting HIV-1 virions attached to the surface of the HIV-1-exposed cells. As the CD4^{hi} GFP⁻ uninfected cells transitioned into CD4^{int} GFP^{lo} cells, the levels

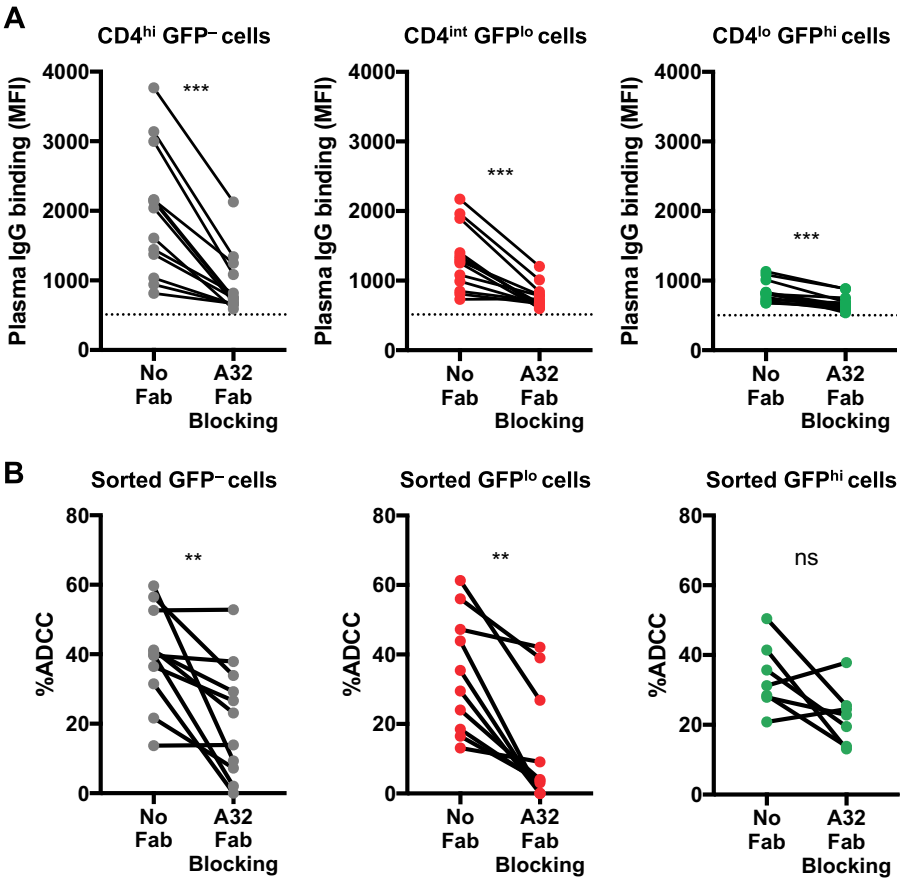

FIG 6 CD4-induced cluster A epitopes are important for HIV-1$^+$ plasma antibody binding and ADCC against HIV-1_{AD8}-infected and uninfected CEM cells. (A) The graphs depict the binding of IgG within HIV-1$^+$ plasma (1:1,000; $n = 13$) to CD4^{hi} GFP$^-$ uninfected cells and to CD4^{int} GFP^{lo} and CD4^{lo} GFP^{hi} infected cells after preincubation with or without A32 Fab (10 μg/ml). The dotted black line depicts plasma IgG binding of an HIV-1-uninfected donor. Plasma IgG binding was determined using flow cytometry, and results are presented as MFI values. (B) ADCC mediated by HIV-1$^+$ plasma antibodies (1:1,000) against HIV-1-infected CEM cells sorted into GFP$^-$ ($n = 11$), GFP^{lo} ($n = 10$), and GFP^{hi} ($n = 7$) populations in the presence or absence of A32 Fab (10 μg/ml). Statistical analyses between matched pairs were performed with a Wilcoxon signed-rank test (ns, not significant; **, $P < 0.01$; ***, $P < 0.001$).

of p24 detected were similar to those of the CD4^{hi} GFP$^-$ cells. In contrast, CD4^{lo} GFP^{hi} cells in the later stages of infection expressed p24 at levels exceeding those of CD4^{hi} GFP$^-$ and CD4^{int} GFP^{lo} cells, most likely as the cells began to produce progeny virions. Thus, these results suggest that a mix of gp120 and viral particles present in the inoculum is sufficient to sensitize uninfected cells to ADCC.

We postulated that the A32- and HIV-1$^+$ plasma IgG binding detected against CD4^{int} GFP^{lo} early infected cells (at 20 h postinfection) could have been due to gp120 or virions from the viral inoculum instead of to newly synthesized Env or gp120 shed from productively infected cells. We therefore performed a time course and measured A32 and PGT126 binding from 12 to 48 h postinfection. A32 binding to uninfected GFP$^-$ bystanders stayed relatively stable (around 6.5- to 7-fold change in MFI over the level of the isotype control) from 12 to 24 h postinfection (Fig. 7B), likely reflecting binding to gp120 or virus particles that originated from the viral inoculum. As for PGT126, the small increase in binding to CD4^{lo} GFP^{hi} infected cells from 18 to 48 h postinfection (1.2- to 1.6-fold over isotype control levels) could reflect binding to low levels of newly synthesized Env (Fig. 7C). A32 binding to the GFP$^-$ bystanders increased greatly from 24 to 48 h (6.5- to 12.1-fold over isotype control levels), whereas binding to CD4^{int} and CD4^{lo} infected cells stayed relatively stable and did not increase over baseline from 18 to 48 h (Fig. 7B). The increasing amount of A32 bound on the surface of uninfected

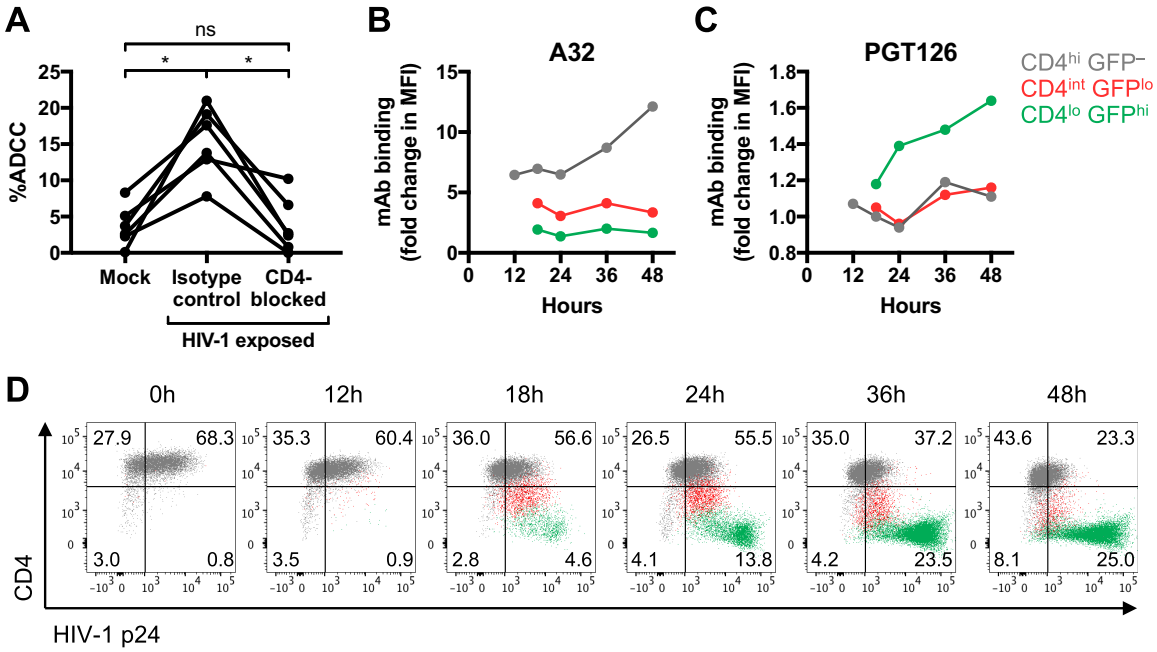

FIG 7 Recognition of CD4^{int} early infected cells by HIV-1^{+} plasma antibodies is due to CD4-bound gp120 or virions that originated from the viral inoculum instead of newly synthesized Env. (A) ADCC mediated by HIV-1^{+} plasma (1:1,000; $n = 6$) against CEM cells exposed to RF10 medium (mock) or HIV-1_{AD8} viral inoculum in the presence of an isotype control or CD4-blocking antibody. CEM cells were preincubated with the mouse isotype control (clone MOPC-21) or anti-CD4 antibody (clone RPA-T4) at 20 μg/ml prior to spinoculation with HIV-1_{AD8}. After spinoculation, the cells were washed and immediately incubated with NK cells and HIV-1^{+} plasma for 5 h (without any prior incubation for viral replication to occur). Statistical analyses between multiple matched groups were performed using a Friedman test followed by Dunn's posttests (ns, not significant; *, $P < 0.05$). (B and C) Binding of A32 and PGT126 at 5 μg/ml to uninfected GFP^{-} bystanders and CD4^{int} GFP^{lo} and CD4^{lo} GFP^{hi} infected cells over time. To normalize MAb binding at each time point, the data are presented as fold change in MFI over the level of the isotype control antibody against influenza virus nucleoprotein (MAb D1-11). The binding to CD4^{int} GFP^{lo} and CD4^{lo} GFP^{hi} infected cells could be assessed only from 18 h onwards as HIV-1_{AD8} (GFP) expression could be detected only after 18 h. (D) Flow cytometry scatter plots of HIV-1_{AD8}-infected CEM cells showing CD4 and HIV-1 p24 expression from 0 to 48 h postinfection. The populations were gated based on CD4 and GFP expression according to the color legend on the figure. The quadrant gates were drawn based on mock-infected cells that were CD4^{hi} and p24^{-} at all time points.

bystander cells from 24 h onwards implies that the productively infected cells in culture were only starting to shed gp120 after 24 h of incubation.

DISCUSSION

In our *in vitro* infection model, we detected higher binding of HIV-1^{+} plasma antibodies to CD4^{int} GFP^{lo} early-stage infected cells than to CD4^{lo} GFP^{hi} late-stage infected cells. This binding was mostly against CD4i epitopes as it was significantly blocked by A32 Fabs, corroborating results from previous studies showing that HIV-1^{+} plasma antibodies predominantly recognize the CD4-bound conformation of Env (6, 7). Our results show that sorted GFP^{lo} infected cells were not more susceptible than sorted GFP^{hi} infected cells to ADCC though it was difficult to determine at which stage the sorted GFP^{lo} cells were killed (CD4^{int} or CD4^{lo}) as they continued to downregulate CD4 and express GFP during the ADCC assay incubation. Sorted GFP^{-} cells that became GFP^{+} during the ADCC assay were more susceptible to ADCC than the cells that remained GFP^{-}, suggesting that early-stage infected cells are better targets for ADCC than uninfected bystander cells coated with gp120.

While it is plausible that CD4i antibodies can eliminate early-stage infected cells in the process of CD4 downregulation, data from the antibody-binding time course experiments suggest that these initial results could be tempered by the complicated nature of infecting cells with HIV-1 *in vitro*. We observed that uninfected GFP^{-} bystander cells had similar levels of A32 binding from 12 to 24 h postinfection but that levels increased 2-fold from 24 to 48 h postinfection (Fig. 7B). Since GFP expression was not detectable at 12 h postinfection in that experiment, the A32 binding detected at

12 h was against CD4-bound gp120 or virions that originated from the initial viral inoculum. That is, HIV-1 gp120- or virion-coated uninfected bystander cells are generated not only during a culture of HIV-1 infection, as previously reported (13, 14), but also through the simple addition of a viral inoculum. The increase in A32 binding to GFP$^-$ bystanders from 24 to 48 h implies that the productively infected cells in culture (most likely GFP^{hi}) were shedding gp120 from 24 h onwards, which is similar to previous observations (13). This led to an accumulation of shed gp120 and virions attached to CD4 on uninfected bystander cells, thereby increasing the level of CD4i epitopes available for A32 binding from 24 to 48 h. This time frame is in agreement with a previous study showing that virus production begins approximately 24 h postinfection (20). Since our earlier assays with HIV-1-infected CEM cells had been performed at 20 h postinfection, the CD4^{int} GFP^{lo} early-stage infected cells most likely had CD4-bound gp120 or virions that originated from the viral inoculum instead of newly synthesized Env. We observed decreasing amounts of plasma IgG binding with decreasing levels of CD4 (CD4^{hi} GFP$^-$ bystanders $>$ CD4^{int} GFP^{lo} $>$ CD4^{lo} GFP^{hi}) (Fig. 2A). If there was no newly synthesized Env on the surface of the cells at 20 h postinfection, we speculated that the decreasing amount of plasma IgG binding we observed in the experiment shown in Fig. 2A could be due to the downregulation of CD4 along with bound gp120 or virions instead of reduced levels of CD4 interacting with newly synthesized Env. We also showed that HIV-1-exposed cells (spinoculated with HIV-1 for 1 h and washed without any further incubation) could be killed by ADCC prior to viral replication (Fig. 7A). These results were further corroborated by the detection of HIV-1 p24 on the surface of uninfected GFP$^-$ bystander cells at 0 h postinfection, reflecting HIV-1 virions attached to the surface of these cells (Fig. 7D). Therefore, similar to the results with uninfected bystander cells, the plasma IgG binding and ADCC we detected against CD4^{int} GFP^{lo} cells at 20 h postinfection were largely directed against CD4-bound gp120 or virions from the viral inoculum.

These results bring into question whether CD4^{int} early infected cells are a real target *in vivo* or an *in vitro* artifact due to the coating of cells with soluble gp120 and viral particles from the inoculum. Previous studies have examined ADCC mediated by CD4i antibodies against cells pulsed with inactivated virions to mimic CD4i epitopes exposed upon binding of viral Env to CD4 during HIV-1 entry (11, 21–23). CD4i epitopes transiently revealed on cells during HIV-1 entry (preintegration) could present a narrow window of opportunity for CD4i ADCC antibodies to block HIV-1 acquisition (12). However, the high levels of inactivated virions used to pulse target cells in these studies are likely not reflective of HIV-1 transmission *in vivo*, which is usually characterized by the transmission of one founder viral variant (24, 25). Thus, we propose that the *in vitro* susceptibility of HIV-1 entry epitopes to ADCC could largely be artifactual and would correspond to the level of virions used to pulse target cells. As has been suggested for cytotoxic T lymphocytes (26), it is tempting to speculate that CD4i antibodies can kill infected cells after viral entry before the release and dissemination of progeny virions. Passive transfer of the nonneutralizing CD4i A32 MAb, however, was not successful in preventing simian-human immunodeficiency virus (SHIV) infection (27). Nevertheless, A32 reduced the number of transmitted/founder viruses in infected macaques, potentially having some impact on the efficiency of virus infection and/or spread. To circumvent the issue of inoculum-derived gp120 and virions sensitizing target cells to ADCC prior to *de novo* Env expression, the transfection of CD4$^+$ target cells with HIV-1 DNA plasmids could be an alternative approach to examine whether Env is expressed prior to complete CD4 downregulation and whether CD4^{int} Env-expressing cells are more susceptible to ADCC mediated by HIV-1$^+$ plasma antibodies than CD4^{lo} Env-expressing cells.

A potential caveat with using GFP reporter viral constructs is that the GFP gene is often in place of *nef,* with *nef* reintroduced downstream under the control of a wild-type encephalomyocarditis virus (EMCV) IRES instead of the HIV-1 long terminal repeat (LTR) promoter (15, 28). A previous study reported that Nef could be overexpressed when under the control of wild-type EMCV IRES compared to expression in

parental nonreporter viruses (28). As such, CD4 downregulation due to IRES-driven Nef could progress faster than in cells infected with wild-type HIV-1. We note, however, that substantially similar antibody staining results were obtained with a primary infectious molecular clone (CH077.t) expressing physiological levels of Nef (Fig. 3B), suggesting that higher levels of Nef expression do not affect our conclusions. In contrast, a recent study found that certain HIV-1 reporter viral constructs display suboptimal expression of Nef in $CD4^+$ T cells, resulting in poorer CD4 downregulation and a corresponding increased exposure of CD4i ADCC epitopes (29). Thus, it is important to consider Nef expression levels when HIV-1 reporter viruses are selected for use in ADCC assays to avoid a significant bias in ADCC mediated by CD4i antibodies. It should be noted that in wild-type HIV-1 viruses, Nef is expressed early in the viral life cycle while Env and Vpu are expressed later as they are dependent on an accumulation of Rev in the nucleus (30). While Nef internalizes CD4 from the plasma membrane, Vpu targets newly synthesized CD4 at the endoplasmic reticulum, with both pathways leading to the degradation of CD4 (31, 32). The early expression of Nef and the concomitant expression of Vpu along with Env ensure the continuous removal of CD4 on HIV-1-infected cells, starting before Env expression at the cell surface, thereby reducing the exposure of CD4i ADCC epitopes on Env.

In summary, we showed in an *in vitro* experimental system that both $CD4^{int}$ GFP^{lo} early and $CD4^{lo}$ GFP^{hi} late infected cells can be killed by HIV-1-specific ADCC even though there was significantly higher binding of HIV-1^+ plasma antibodies to the $CD4^{int}$ GFP^{lo} cells. The ADCC detected against these early infected cells, however, was largely artifactual due to the high levels of soluble gp120 and virions from the initial viral inoculum binding to CD4, sensitizing the early infected cells to ADCC prior to *de novo* Env expression. As such, future studies examining ADCC against HIV-1 entry epitopes or early-stage infected cells should take into consideration the inherent caveats of *in vitro* infection systems and develop improved models to address the potential *in vivo* role for ADCC against cells with nascent HIV-1 infection.

MATERIALS AND METHODS

Study participants. Whole-blood samples were obtained from 15 HIV-1^+ individuals at the Melbourne Sexual Health Centre. The HIV-1^+ donors had a median age of 50 years (range, 29 to 81 years), were infected for an estimated 96 months (range, 22 to 300 months), were all suppressed on antiretroviral therapy for a median of 84 months (range, 11 to 204 months) with HIV-1 viral loads of $<$200 copies/ml, and had median CD4 counts of 554 cells/mm^3 (range, 200 to 1,006 cells/mm^3). The plasma fraction was removed, heat inactivated at 56°C for 1 h, and stored at −20°C until further use. For the staining of primary $CD4^+$ T cells (Fig. 3B), sera from three HIV-1-infected individuals from the Montreal Primary HIV Infection Cohort and the Canadian Cohort of HIV-infected Slow Progressors were collected, heat inactivated, and stored as previously described (6). Whole blood was also collected from HIV-1-uninfected healthy donors for the isolation of effector NK cells and target $CD4^+$ T cells. Peripheral blood mononuclear cells (PBMCs) were isolated from whole blood via Ficoll-Paque density gradient centrifugation (GE Healthcare). NK cells were enriched from freshly isolated PBMCs with an EasySep Human NK Cell Enrichment kit (Stemcell Technologies). $CD4^+$ T cells were enriched from cryopreserved PBMCs with an EasySep Human $CD4^+$ T cell enrichment kit (Stemcell Technologies). Informed consent was obtained prior to collection of blood samples, and the described studies were approved by the relevant human ethics committees.

Antibodies and cell lines. An array of MAbs against HIV-1 gp120 (A32, 2G12, PGT126, PGT145, and 3BNC117) and the TZM-bl and CEM.NKr-CCR5 (CEM) cell lines were obtained from the NIH AIDS Reagent Program. The anti-gp120-gp41 interface MAb PGT151 was kindly provided by the International AIDS Vaccine Initiative. These Env-specific MAbs have been previously assessed for binding or neutralization of the Env variants (AD8, ADA, and CH077.t) used in the antibody staining assays (10, 14, 33, 34). The MAb against influenza virus nucleoprotein (D1-11) (17) was kindly provided by Adam Wheatley (University of Melbourne, Melbourne, Australia) and used as an isotype control for the staining of Env-specific MAbs.

Fab production. To generate A32 Fabs, A32 IgG was first produced by transient transfection of A32 heavy- and light-chain plasmids into Freestyle 293-F cells (Invitrogen). First, A32 heavy- and light-chain plasmids (125 μg) were added to 25 ml of Opti-MEM reduced-serum medium (Gibco). Next, 0.5 ml of XtremeGENE HP transfection reagent (Roche) was added dropwise to the mixture and incubated at room temperature for 30 min. The DNA and transfection reagent were then added to 500 ml of 293-F cells (1×10^6 cells/ml) in Freestyle expression medium. After 6 to 7 days of incubation at 37°C with 8% CO_2, cells were pelleted by centrifugation, and the supernatant was filtered through a 0.2-μm-pore-size filter. A32 IgG was then purified by passing the supernatant over a HiTrap protein A column (GE Healthcare) equilibrated with phosphate-buffered saline (PBS), pH 7.2. After the column was washed with PBS, IgG was eluted with 0.1 M glycine, pH 3.0, and immediately diluted 10:1 with 1 M Tris-HCl, pH 8.5, to raise the

pH. Eluted protein was concentrated to approximately 10 mg/ml, and the buffer was exchanged for PBS, pH 7.2.

A32 Fabs were generated from purified IgG by papain cleavage. A32 IgG in PBS was first exchanged to Fab digest buffer (10 mM sodium phosphate and 5 mM cysteine, pH 7.0) and added to 1 ml of papain-linked agarose slurry (Thermo Fisher) at approximately 10 mg/ml. The digest was incubated at 37°C overnight, pelleted by centrifugation, and filtered to remove papain. Digested protein was passed over a protein A column (GE Healthcare) equilibrated in PBS, pH 7.2, to remove cleaved Fc and undigested A32 IgG. Flowthrough fractions containing Fabs were concentrated and loaded on a Superdex 200 gel filtration column (GE Healthcare) equilibrated in 25 mM Tris-HCl, pH 8.5, and 150 mM sodium chloride. The Fab elution peak corresponding to a molecular weight of approximately 50 kDa was collected and concentrated prior to use in experiments.

Virus production and infection. For infection of the CD4$^+$ T cell line (CEM cells) used in the experiments shown in Fig. 1, 2, 4, 5, 6, and 7, the GFP reporter HIV-1$_{AD8}$ strain was utilized. Plasmid DNA encoding an NL4.3 backbone with AD8 Env and enhanced GFP (EGFP) inserted one base downstream of the *env* open reading frame (15), followed by an IRES-Nef coding sequence, was transiently transfected into HEK293T cells using calcium phosphate as previously described (35). Briefly, virus-containing supernatant was collected after 2 days, filtered (0.45-μm pore size), and concentrated by ultracentrifugation through 20% sucrose. Viral pellets were resuspended in a 75-fold-smaller volume, and aliquots were stored at −80°C. To normalize virus stocks, the 50% tissue culture infectious doses (TCID$_{50}$) were determined by limiting dilution in TZM-bl cells using luciferase as a readout for infection (Luciferase Assay System; Promega). CEM cells were infected with the GFP reporter HIV-1$_{AD8}$ strain at a multiplicity of infection (MOI) of 0.5 to 2 in 96-well plates by spinoculation at 1,200 × *g* for 1 h at 21°C. Infected CEM cells were then incubated at 37°C with 5% CO_2 for 20 h and washed once before use in assays. For time course experiments, infected CEM cells were incubated for 12, 18, 24, 36, and 48 h postspinoculation before use in assays. For some infection conditions, the fusion inhibitor T20 (Roche) was added at 10 μg/ml before or 4 h after spinoculation with HIV-1$_{AD8}$.

For the infection of primary CD4$^+$ T cells in the experiment shown in Fig. 3, vesicular stomatitis virus G protein (VSV-G) pseudotyped HIV-1 strains were used. The GFP reporter HIV-1$_{ADA}$ strain was produced with the pNL4.3(ADA)-GFP.IRES.Nef plasmid containing intact or defective *nef* and *vpu* genes as previously described (6, 9). Similarly, the transmitted/founder HIV-1 infectious molecular clone CH077.t (GenBank accession number JN944941) was produced using plasmids containing intact or defective *nef* and *vpu* genes as previously described (36–39). CH077.t HIV-1 defective for Nef and Vpu expression was generated by introducing two stop codons directly after the start codons of *nef* and *vpu* (40). VSV-G pseudotyping was used to achieve similar levels of infection between the wild-type and Nef- and Vpu-deleted viruses. This pseudotyping did not affect HIV-1 Env expression or the recognition of infected cells by A32 or HIV-1$^+$ serum (data not shown). Prior to infection, primary CD4$^+$ T cells were activated with phytohemagglutinin-L (10 μg/ml) for 48 h and maintained in RF20 medium (RPMI 1640 medium supplemented with 20% fetal bovine serum and 1% penicillin–streptomycin–L-glutamine) in the presence of recombinant interleukin-2 (IL-2; 100 U/ml). The activated primary CD4$^+$ T cells were then infected with the GFP reporter HIV-1$_{ADA}$ strain or CH077.t HIV-1 in 96-well plates by spinoculation at 800 × *g* for 1 h at 25°C. HIV-1$_{ADA}$-infected cells were incubated for 48 h while CH077.t HIV-1-infected cells were incubated for 18 h prior to use in assays.

Flow cytometric analysis of HIV-1-infected cells. CEM cells infected with the GFP reporter HIV-1$_{AD8}$ strain were incubated with HIV-1$^+$ plasma samples (1:1,000 dilution) or Env-specific MAbs (5 μg/ml) for 30 min at room temperature. To block CD4i epitopes, the infected cells were preincubated with A32 Fab at 10 μg/ml for 15 min at room temperature and washed prior to the addition of HIV-1$^+$ plasma. The binding of HIV-1$^+$ plasma antibodies was then assessed with an allophycocyanin (APC)-conjugated secondary mouse anti-human IgG Fc antibody (1:200 dilution) (clone HP6017; BioLegend), while the binding of Env-specific monoclonal antibodies was assessed with an Alexa Fluor 647 (AF647)-conjugated secondary goat anti-human IgG antibody (1:1,000 dilution; Thermo Fisher Scientific). Cells were concurrently stained with brilliant violet 605 (BV605)-conjugated anti-CD4 antibody (clone OKT4; BioLegend) for 30 min at room temperature. For the detection of HIV-1 virions on the surface of HIV-1-exposed cells and intracellular HIV-1 p24 expression in infected cells, cells were fixed with 1% formaldehyde and permeabilized with 1× fluorescence-activated cell sorting (FACS) permeabilization buffer (BD) prior to staining with the phycoerythrin (PE)-conjugated anti-p24 antibody (1:1,250 dilution) (clone KC57; Beckman Coulter). Finally, cells were fixed with 1% formaldehyde and acquired on an LSRFortessa flow cytometer (BD).

Primary CD4$^+$ T cells infected with the GFP reporter HIV-1$_{ADA}$ strain and the transmitted/founder HIV-1 infectious molecular clone CH077.t were incubated with BV421-conjugated anti-CD4 antibody (clone OKT4; BioLegend) and HIV-1$^+$ serum samples (1:1,000 dilution) or Env-specific MAbs (5 μg/ml) for 30 min at room temperature. Cells were then stained with AF647-conjugated goat anti-human secondary antibody (1 μg/ml; Thermo Fisher Scientific) for 15 min at room temperature. Viability of the primary cells was determined via staining with AquaVivid viability dye (Thermo Fisher Scientific). Next, as a measure of HIV-1 infection, cells infected with CH077.t were fixed and permeabilized with a Cytofix/Cytoperm Fixation/Permeabilization kit (BD) prior to intracellular staining for HIV-1 p24 using PE-conjugated anti-p24 antibody (1:100 dilution) (clone KC57; Beckman Coulter). Last, both cells infected with the GFP reporter HIV-1$_{ADA}$ strain and those infected with CH077.t were fixed with 2% formaldehyde and acquired on an LSRII flow cytometer.

Infected cell elimination ADCC assay. A modified version of the infected-cell elimination assay (41) was performed to assess killing of HIV-1-infected cells mediated by antibodies within HIV-1$^+$ plasma. At

20 h postinfection, CEM cells infected with the GFP reporter HIV-1_{AD8} strain were stained with the viability dye Live/Dead Near-IR (Life Technologies) and sorted into GFP^-, GFP^{lo}, and GFP^{hi} populations with a FACSAria III cell sorter (BD). Effector NK cells were purified from HIV-1-uninfected donor PBMCs and stained with the cell proliferation dye eFluor 450 (eBioscience). The effector NK and target CEM cells were incubated at a 5:1 effector/target ratio in the presence of $HIV\text{-}1^+$/$HIV\text{-}1^-$ plasma (1:1,000 dilution) or no plasma. The cells were then centrifuged for 1 min at 300 × g and incubated at 37°C with 5% CO_2 for 5 h. For the A32 Fab blocking conditions, the infected target cells were preincubated with A32 Fab at 10 μg/ml for 15 min at room temperature prior to the addition of $HIV\text{-}1^+$ plasma or effector NK cells. After 5 h, a fixed number of uninfected CEM cells stained with eFluor 670 cell proliferation dye (eBioscience) was added into each sample as a reference population to calculate relative percent ADCC of the target cells. The samples were then washed and stained with the viability dye Live/Dead Near-IR (Life Technologies) and BV605-conjugated anti-CD4 antibody (clone OKT4). After a final wash, the cells were fixed with 1% formaldehyde and analyzed on an LSRFortessa flow cytometer (BD). Percent ADCC was calculated using the following formula: percent target cells in ([targets + effectors] − [targets + effectors + plasma]) ÷ targets only × 100.

For the experiments examining ADCC against HIV-1-exposed cells, CEM cells were preincubated with an anti-CD4 antibody that blocks gp120 binding (clone RPA-T4; BioLegend) or a mouse isotype control (clone MOPC-21; BioLegend) at 20 μg/ml for 30 min prior to spinoculation with HIV-1_{AD8} at 1,200 × *g* and 21°C for 1 h. After spinoculation, the cells were washed and immediately used as target cells for the ADCC assay without any further incubation for viral replication to occur.

Statistics. Statistical analyses were performed with GraphPad Prism, version 7. Comparisons between matched groups were analyzed using a nonparametric Wilcoxon signed-rank test. Comparisons between multiple matched groups were analyzed using a nonparametric Friedman test with Dunn's multiple-comparison posttest. *P* values of less than 0.05 were considered significant. Statistics in the manuscript are presented in the following format: (median [interquartile range] versus median [interquartile range]; *P* value of statistical test).

ACKNOWLEDGMENTS

We thank all subjects for their participation. We thank Damian Purcell (University of Melbourne, Melbourne, Australia) and Yasuko Tsunetsugu-Yokota (National Institute of Infectious Diseases, Tokyo, Japan) for providing us with the GFP reporter HIV-1_{AD8} virus.

This work was supported by a National Health and Medical Research Council Program Grant to S.J.K. This work was also supported by CIHR foundation grant 352417 to A.F. A.F. is the recipient of a Canada Research Chair on Retroviral Entry (grant RCHS0235). J.R. is the recipient of a Mathilde Krim Fellowship in Basic Biomedical Research from amfAR. J.P. is the recipient of a CIHR PhD fellowship award. The funders had no role in study design, data collection and analysis, decision to publish, or preparation of the manuscript.

The views expressed in the manuscript are those of the authors and do not reflect the official policy or position of the Uniformed Services University, the U.S. Army, the Department of Defense, or the U.S. Government.

We declare that we have no competing interests.

REFERENCES

1. Haynes BF, Gilbert PB, McElrath MJ, Zolla-Pazner S, Tomaras GD, Alam SM, Evans DT, Montefiori DC, Karnasuta C, Sutthent R, Liao HX, DeVico AL, Lewis GK, Williams C, Pinter A, Fong Y, Janes H, DeCamp A, Huang Y, Rao M, Billings E, Karasavvas N, Robb ML, Ngauy V, de Souza MS, Paris R, Ferrari G, Bailer RT, Soderberg KA, Andrews C, Berman PW, Frahm N, De Rosa SC, Alpert MD, Yates NL, Shen X, Koup RA, Pitisuttithum P, Kaewkungwal J, Nitayaphan S, Rerks-Ngarm S, Michael NL, Kim JH. 2012. Immune-correlates analysis of an HIV-1 vaccine efficacy trial. N Engl J Med 366:1275–1286. https://doi.org/10.1056/NEJMoa1113425.
2. Alpert MD, Harvey JD, Lauer WA, Reeves RK, Piatak M, Jr, Carville A, Mansfield KG, Lifson JD, Li W, Desrosiers RC, Johnson RP, Evans DT. 2012. ADCC develops over time during persistent infection with live-attenuated SIV and is associated with complete protection against SIV(mac)251 challenge. PLoS Pathog 8:e1002890. https://doi.org/10.1371/journal.ppat.1002890.
3. Lambotte O, Ferrari G, Moog C, Yates NL, Liao HX, Parks RJ, Hicks CB, Owzar K, Tomaras GD, Montefiori DC, Haynes BF, Delfraissy JF. 2009. Heterogeneous neutralizing antibody and antibody-dependent cell cytotoxicity responses in HIV-1 elite controllers. AIDS 23:897–906. https://doi.org/10.1097/QAD.0b013e328329f97d.
4. Banks ND, Kinsey N, Clements J, Hildreth JE. 2002. Sustained antibody-dependent cell-mediated cytotoxicity (ADCC) in SIV-infected macaques correlates with delayed progression to AIDS. AIDS Res Hum Retroviruses 18:1197–1205. https://doi.org/10.1089/08892220260387940.
5. Gomez-Roman VR, Patterson LJ, Venzon D, Liewehr D, Aldrich K, Florese R, Robert-Guroff M. 2005. Vaccine-elicited antibodies mediate antibody-dependent cellular cytotoxicity correlated with significantly reduced acute viremia in rhesus macaques challenged with SIVmac251. J Immunol 174:2185–2189. https://doi.org/10.4049/jimmunol.174.4.2185.
6. Veillette M, Coutu M, Richard J, Batraville LA, Dagher O, Bernard N, Tremblay C, Kaufmann DE, Roger M, Finzi A. 2015. The HIV-1 gp120 CD4-bound conformation is preferentially targeted by antibody-dependent cellular cytotoxicity-mediating antibodies in sera from HIV-1-infected individuals. J Virol 89:545–551. https://doi.org/10.1128/JVI.02868-14.
7. Williams KL, Cortez V, Dingens AS, Gach JS, Rainwater S, Weis JF, Chen X, Spearman P, Forthal DN, Overbaugh J. 2015. HIV-specific CD4-induced antibodies mediate broad and potent antibody-dependent cellular cytotoxicity activity and are commonly detected in plasma from HIV-infected humans. EBioMedicine 2:1464–1477. https://doi.org/10.1016/j.ebiom.2015.09.001.
8. Bonsignori M, Pollara J, Moody MA, Alpert MD, Chen X, Hwang KK,

Gilbert PB, Huang Y, Gurley TC, Kozink DM, Marshall DJ, Whitesides JF, Tsao CY, Kaewkungwal J, Nitayaphan S, Pitisuttithum P, Rerks-Ngarm S, Kim JH, Michael NL, Tomaras GD, Montefiori DC, Lewis GK, DeVico A, Evans DT, Ferrari G, Liao HX, Haynes BF. 2012. Antibody-dependent cellular cytotoxicity-mediating antibodies from an HIV-1 vaccine efficacy trial target multiple epitopes and preferentially use the VH1 gene family. J Virol 86:11521–11532. https://doi.org/10.1128/JVI.01023-12.

9. Veillette M, Desormeaux A, Medjahed H, Gharsallah N-E, Coutu M, Baalwa J, Guan Y, Lewis G, Ferrari G, Hahn BH, Haynes BF, Robinson JE, Kaufmann DE, Bonsignori M, Sodroski J, Finzi A, Silvestri G. 2014. Interaction with cellular CD4 exposes HIV-1 envelope epitopes targeted by antibody-dependent cell-mediated cytotoxicity. J Virol 88:2633–2644. https://doi.org/10.1128/JVI.03230-13.
10. Ding S, Veillette M, Coutu M, Prevost J, Scharf L, Bjorkman PJ, Ferrari G, Robinson JE, Sturzel C, Hahn BH, Sauter D, Kirchhoff F, Lewis GK, Pazgier M, Finzi A. 2016. A highly conserved residue of the HIV-1 gp120 inner domain is important for antibody-dependent cellular cytotoxicity responses mediated by anti-cluster A antibodies. J Virol 90:2127–2134. https://doi.org/10.1128/JVI.02779-15.
11. Guan Y, Pazgier M, Sajadi MM, Kamin-Lewis R, Al-Darmarki S, Flinko R, Lovo E, Wu X, Robinson JE, Seaman MS, Fouts TR, Gallo RC, DeVico AL, Lewis GK. 2013. Diverse specificity and effector function among human antibodies to HIV-1 envelope glycoprotein epitopes exposed by CD4 binding. Proc Natl Acad Sci U S A 110:E69–E78. https://doi.org/10.1073/pnas.1217609110.
12. Lewis GK, Guan Y, Kamin-Lewis R, Sajadi M, Pazgier M, Devico AL. 2014. Epitope target structures of Fc-mediated effector function during HIV-1 acquisition. Curr Opin HIV AIDS 9:263–270. https://doi.org/10.1097/COH.0000000000000055.
13. Richard J, Veillette M, Ding S, Zoubchenok D, Alsahafi N, Coutu M, Brassard N, Park J, Courter JR, Melillo B, Smith AB, III, Shaw GM, Hahn BH, Sodroski J, Kaufmann DE, Finzi A. 2016. Small CD4 mimetics prevent HIV-1 uninfected bystander $CD4^+$ T cell killing mediated by antibody-dependent cell-mediated cytotoxicity. EBioMedicine 3:122–134. https://doi.org/10.1016/j.ebiom.2015.12.004.
14. Richard J, Prevost J, Baxter AE, von Bredow B, Ding S, Medjahed H, Delgado GG, Brassard N, Sturzel CM, Kirchhoff F, Hahn BH, Parsons MS, Kaufmann DE, Evans DT, Finzi A. 2018. Uninfected bystander cells impact the measurement of HIV-specific antibody-dependent cellular cytotoxicity responses. mBio 9:e00358-18. https://doi.org/10.1128/mBio.00358-18.
15. Yamamoto T, Tsunetsugu-Yokota Y, Mitsuki YY, Mizukoshi F, Tsuchiya T, Terahara K, Inagaki Y, Yamamoto N, Kobayashi K, Inoue J. 2009. Selective transmission of R5 HIV-1 over X4 HIV-1 at the dendritic cell-T cell infectious synapse is determined by the T cell activation state. PLoS Pathog 5:e1000279. https://doi.org/10.1371/journal.ppat.1000279.
16. Tolbert WD, Gohain N, Veillette M, Chapleau JP, Orlandi C, Visciano ML, Ebadi M, DeVico AL, Fouts TR, Finzi A, Lewis GK, Pazgier M. 2016. Paring down HIV Env: design and crystal structure of a stabilized inner domain of HIV-1 gp120 displaying a major ADCC target of the A32 region. Structure 24:697–709. https://doi.org/10.1016/j.str.2016.03.005.
17. Wrammert J, Smith K, Miller J, Langley WA, Kokko K, Larsen C, Zheng NY, Mays I, Garman L, Helms C, James J, Air GM, Capra JD, Ahmed R, Wilson PC. 2008. Rapid cloning of high-affinity human monoclonal antibodies against influenza virus. Nature 453:667–671. https://doi.org/10.1038/nature06890.
18. Trkola A, Purtscher M, Muster T, Ballaun C, Buchacher A, Sullivan N, Srinivasan K, Sodroski J, Moore JP, Katinger H. 1996. Human monoclonal antibody 2G12 defines a distinctive neutralization epitope on the gp120 glycoprotein of human immunodeficiency virus type 1. J Virol 70:1100–1108.
19. Ferrari G, Pollara J, Kozink D, Harms T, Drinker M, Freel S, Moody MA, Alam SM, Tomaras GD, Ochsenbauer C, Kappes JC, Shaw GM, Hoxie JA, Robinson JE, Haynes BF. 2011. An HIV-1 gp120 envelope human monoclonal antibody that recognizes a C1 conformational epitope mediates potent antibody-dependent cellular cytotoxicity (ADCC) activity and defines a common ADCC epitope in human HIV-1 serum. J Virol 85:7029–7036. https://doi.org/10.1128/JVI.00171-11.
20. Kim SY, Byrn R, Groopman J, Baltimore D. 1989. Temporal aspects of DNA and RNA synthesis during human immunodeficiency virus infection: evidence for differential gene expression. J Virol 63:3708–3713.
21. Gohain N, Tolbert WD, Acharya P, Yu L, Liu T, Zhao P, Orlandi C, Visciano ML, Kamin-Lewis R, Sajadi MM, Martin L, Robinson JE, Kwong PD, DeVico AL, Ray K, Lewis GK, Pazgier M. 2015. Cocrystal structures of antibody N60-i3 and antibody JR4 in complex with gp120 define more cluster A epitopes involved in effective antibody-dependent effector function against HIV-1. J Virol 89:8840–8854. https://doi.org/10.1128/JVI.01232-15.
22. Huang Y, Ferrari G, Alter G, Forthal DN, Kappes JC, Lewis GK, Love JC, Borate B, Harris L, Greene K, Gao H, Phan TB, Landucci G, Goods BA, Dowell KG, Cheng HD, Bailey-Kellogg C, Montefiori DC, Ackerman ME. 2016. Diversity of antiviral IgG effector activities observed in HIV-infected and vaccinated subjects. J Immunol 197:4603–4612. https://doi.org/10.4049/jimmunol.1601197.
23. Orlandi C, Flinko R, Lewis GK. 2016. A new cell line for high throughput HIV-specific antibody-dependent cellular cytotoxicity (ADCC) and cell-to-cell virus transmission studies. J Immunol Methods 433:51–58. https://doi.org/10.1016/j.jim.2016.03.002.
24. Keele BF, Giorgi EE, Salazar-Gonzalez JF, Decker JM, Pham KT, Salazar MG, Sun C, Grayson T, Wang S, Li H, Wei X, Jiang C, Kirchherr JL, Gao F, Anderson JA, Ping LH, Swanstrom R, Tomaras GD, Blattner WA, Goepfert PA, Kilby JM, Saag MS, Delwart EL, Busch MP, Cohen MS, Montefiori DC, Haynes BF, Gaschen B, Athreya GS, Lee HY, Wood N, Seoighe C, Perelson AS, Bhattacharya T, Korber BT, Hahn BH, Shaw GM. 2008. Identification and characterization of transmitted and early founder virus envelopes in primary HIV-1 infection. Proc Natl Acad Sci U S A 105:7552–7557. https://doi.org/10.1073/pnas.0802203105.
25. Abrahams MR, Anderson JA, Giorgi EE, Seoighe C, Mlisana K, Ping LH, Athreya GS, Treurnicht FK, Keele BF, Wood N, Salazar-Gonzalez JF, Bhattacharya T, Chu H, Hoffman I, Galvin S, Mapanje C, Kazembe P, Thebus R, Fiscus S, Hide W, Cohen MS, Karim SA, Haynes BF, Shaw GM, Hahn BH, Korber BT, Swanstrom R, Williamson C, for the CAPRISA Acute Infection Study Team and the Center for HIV-AIDS Vaccine Immunology Consortium. 2009. Quantitating the multiplicity of infection with human immunodeficiency virus type 1 subtype C reveals a non-Poisson distribution of transmitted variants. J Virol 83:3556–3567. https://doi.org/10.1128/JVI.02132-08.
26. Sacha JB, Chung C, Rakasz EG, Spencer SP, Jonas AK, Bean AT, Lee W, Burwitz BJ, Stephany JJ, Loffredo JT, Allison DB, Adnan S, Hoji A, Wilson NA, Friedrich TC, Lifson JD, Yang OO, Watkins DI. 2007. Gag-specific $CD8^+$ T lymphocytes recognize infected cells before AIDS-virus integration and viral protein expression. J Immunol 178:2746–2754. https://doi.org/10.4049/jimmunol.178.5.2746.
27. Santra S, Tomaras GD, Warrier R, Nicely NI, Liao HX, Pollara J, Liu P, Alam SM, Zhang R, Cocklin SL, Shen X, Duffy R, Xia SM, Schutte RJ, Pemble Iv CW, Dennison SM, Li H, Chao A, Vidnovic K, Evans A, Klein K, Kumar A, Robinson J, Landucci G, Forthal DN, Montefiori DC, Kaewkungwal J, Nitayaphan S, Pitisuttithum P, Rerks-Ngarm S, Robb ML, Michael NL, Kim JH, Soderberg KA, Giorgi EE, Blair L, Korber BT, Moog C, Shattock RJ, Letvin NL, Schmitz JE, Moody MA, Gao F, Ferrari G, Shaw GM, Haynes BF. 2015. Human non-neutralizing HIV-1 envelope monoclonal antibodies limit the number of founder viruses during SHIV mucosal infection in rhesus macaques. PLoS Pathog 11:e1005042. https://doi.org/10.1371/journal.ppat.1005042.
28. Alberti MO, Jones JJ, Miglietta R, Ding H, Bakshi RK, Edmonds TG, Kappes JC, Ochsenbauer C. 2015. Optimized replicating Renilla luciferase reporter HIV-1 utilizing novel internal ribosome entry site elements for native Nef expression and function. AIDS Res Hum Retroviruses 31:1278–1296. https://doi.org/10.1089/aid.2015.0074.
29. Prevost J, Richard J, Medjahed H, Alexander A, Jones J, Kappes JC, Ochsenbauer C, Finzi A. 2018. Incomplete downregulation of CD4 expression affects HIV-1 Env conformation and antibody-dependent cellular cytotoxicity responses. J Virol 92:e00484-18. https://doi.org/10.1128/JVI.00484-18.
30. Frankel AD, Young JA. 1998. HIV-1: fifteen proteins and an RNA. Annu Rev Biochem 67:1–25. https://doi.org/10.1146/annurev.biochem.67.1.1.
31. Schwartz O, Dautry-Varsat A, Goud B, Marechal V, Subtil A, Heard JM, Danos O. 1995. Human immunodeficiency virus type 1 Nef induces accumulation of CD4 in early endosomes. J Virol 69:528–533.
32. Willey RL, Maldarelli F, Martin MA, Strebel K. 1992. Human immunodeficiency virus type 1 Vpu protein induces rapid degradation of CD4. J Virol 66:7193–7200.
33. Boyd DF, Peterson D, Haggarty BS, Jordan AP, Hogan MJ, Goo L, Hoxie JA, Overbaugh J. 2015. Mutations in HIV-1 envelope that enhance entry with the macaque CD4 receptor alter antibody recognition by disrupting quaternary interactions within the trimer. J Virol 89:894–907. https://doi.org/10.1128/JVI.02680-14.

34. von Bredow B, Arias JF, Heyer LN, Moldt B, Le K, Robinson JE, Zolla-Pazner S, Burton DR, Evans DT. 2016. Comparison of antibody-dependent cell-mediated cytotoxicity and virus neutralization by HIV-1 Env-specific monoclonal antibodies. J Virol 90:6127–6139. https://doi.org/10.1128/JVI.00347-16.
35. Das AT, Klaver B, Klasens BI, van Wamel JL, Berkhout B. 1997. A conserved hairpin motif in the R-U5 region of the human immunodeficiency virus type 1 RNA genome is essential for replication. J Virol 71:2346–2356.
36. Ochsenbauer C, Edmonds TG, Ding H, Keele BF, Decker J, Salazar MG, Salazar-Gonzalez JF, Shattock R, Haynes BF, Shaw GM, Hahn BH, Kappes JC. 2012. Generation of transmitted/founder HIV-1 infectious molecular clones and characterization of their replication capacity in CD4 T lymphocytes and monocyte-derived macrophages. J Virol 86:2715–2728. https://doi.org/10.1128/JVI.06157-11.
37. Richard J, Veillette M, Brassard N, Iyer SS, Roger M, Martin L, Pazgier M, Schon A, Freire E, Routy JP, Smith AB, III, Park J, Jones DM, Courter JR, Melillo BN, Kaufmann DE, Hahn BH, Permar SR, Haynes BF, Madani N, Sodroski JG, Finzi A. 2015. CD4 mimetics sensitize HIV-1-infected cells to ADCC. Proc Natl Acad Sci U S A 112:E2687–E2694. https://doi.org/10.1073/pnas.1506755112.
38. Bar KJ, Tsao CY, Iyer SS, Decker JM, Yang Y, Bonsignori M, Chen X, Hwang KK, Montefiori DC, Liao HX, Hraber P, Fischer W, Li H, Wang S, Sterrett S, Keele BF, Ganusov VV, Perelson AS, Korber BT, Georgiev I, McLellan JS, Pavlicek JW, Gao F, Haynes BF, Hahn BH, Kwong PD, Shaw GM. 2012. Early low-titer neutralizing antibodies impede HIV-1 replication and select for virus escape. PLoS Pathog 8:e1002721. https://doi.org/10.1371/journal.ppat.1002721.
39. Fenton-May AE, Dibben O, Emmerich T, Ding H, Pfafferott K, Aasa-Chapman MM, Pellegrino P, Williams I, Cohen MS, Gao F, Shaw GM, Hahn BH, Ochsenbauer C, Kappes JC, Borrow P. 2013. Relative resistance of HIV-1 founder viruses to control by interferon-alpha. Retrovirology 10:146. https://doi.org/10.1186/1742-4690-10-146.
40. Heigele A, Kmiec D, Regensburger K, Langer S, Peiffer L, Sturzel CM, Sauter D, Peeters M, Pizzato M, Learn GH, Hahn BH, Kirchhoff F. 2016. The potency of Nef-mediated SERINC5 antagonism correlates with the prevalence of primate lentiviruses in the wild. Cell Host Microbe 20:381–391. https://doi.org/10.1016/j.chom.2016.08.004.
41. Richard J, Veillette M, Batraville LA, Coutu M, Chapleau JP, Bonsignori M, Bernard N, Tremblay C, Roger M, Kaufmann DE, Finzi A. 2014. Flow cytometry-based assay to study HIV-1 gp120 specific antibody-dependent cellular cytotoxicity responses. J Virol Methods 208:107–114. https://doi.org/10.1016/j.jviromet.2014.08.003.